Journal of Physics: Conference Series **712** (2016) 012048 doi:10.1088/1742-6596/712/1/012048

Atomic structure of PtCu nanoparticles in PtCu/C catalysts prepared by simultaneous and sequential deposition of components on carbon support

L A Bugaev, V V Srabionyan, V V Pryadchenko, A L Bugaev, L A Avakyan, S V Belenov and V E Guterman
Southern Federal University, Physical and Chemical Faculties, 344090, Zorge str. 5, Rostov-on-Don, Russia

E-mail: bugaev@sfedu.ru

Abstract. Nanocatalysts PtCu/C with different distribution of components in bimetallic PtCu nanoparticles (NPs) were synthesized by simultaneous and sequential deposition of Cu and Pt on carbon support. Electrochemical stability of the obtained samples PtCu/C was studied using the cyclic voltammetry. Characterization of atomic structure of as prepared PtCu NPs and obtained after acid treatment was performed by Pt L_3- and Cu K-edge EXAFS using the technique for determining local structure parameters of the absorbing atom under strong correlations among them. EXAFS derived parameters were used for generation of structural models of PtCu NPs by the method of cluster simulations. Within this approach, the models of atomic structure of PtCu NPs obtained by the two methods of synthesis, before and after post treatment and after two months from their preparation were revealed.

1. Introduction

Besides of other valuable applications, the platinum NPs on carbon supports are a basic component of catalytic layers in low-temperature fuel cells. The main reasons that prevent commercial use of these materials are relatively high cost and insufficient corrosive and morphological stability of NPs during the operation. An efficient way to overcome these problems is the synthesis of catalytic layer containing bimetallic NPs of core-shell architecture, with a core of transition metal (Me) atoms and a shell of Pt atoms. For such architecture, the decisive factors determining the catalytic properties of bimetallic NPs are the thickness, composition and continuity of the shell, its atomic structure, shape, surface morphology, stability of the "core-shell" structure in time and during operation.

Despite the progress in synthesis and applications of bimetallic PtMe NPs with the "core-shell" architecture [1,2], the development of reliable and technological methods for the production of catalysts containing large amounts of core-shell NPs on the carbon supports remains a challenging problem. The development of these methods requires in turn the improvement of the methods for diagnostics of NPs atomic structure, which enable to reveal the high concentration of Pt atoms in the near-surface region of NPs – necessary (but not sufficient) condition for high adsorption and catalytic activities of PtMe/C electrocatalysts.

2. Experimental results

In this work PtCu/C nanocatalysts were synthesized by two different approaches: simultaneous (obtained samples are referred to as PtCu_sim/C) and sequential (PtCu_seq/C) chemical reduction of

Cu^{2+} ($CuSO_4$) and Pt (IV) (H_2PtCl_6) in a carbon (Vulcan XC-72, Cabot) suspension based on a two-component water-organic solvent at pH = 10 (excess of NH_3). In the case of sequential reduction, first, nanostructured material Cu/C was obtained by the reduction of Cu^{2+} and, then, without removing of Cu/C from the solution, a certain amount of an aqueous solution of H_2PtCl_6 containing an excess of NH_3 was added. In the case of simultaneous deposition the metals reduction was performed from a solution containing a mixture of platinum and copper compounds. It is reasonable to assume that the metal component in the resultant PtCu/C catalyst should have the structure of a PtCu solid solution [3]. A part of the resulting PtCu/C catalyst was exposed to post-treatment: the materials were maintained at room temperature (RT) in 1 M nitric acid for 1 hour and then washed and dried. The corresponding materials are referred to as PtCu_sim-at/C and PtCu_seq-at/C respectively.

XRD study of synthesized materials showed, that PtCu_sim/C and PtCu_sim-at/C contain only one phase corresponding to PtCu solid solution, while PtCu_seq/C and PtCu_seq-at/C contain phases of Pt and Cu. These two phases can exist both in the core-shell NPs and as separate Pt and Cu NPs. Copper oxide, which probably exists in all samples according to EXAFS data, is amorphous and therefore is not seen as a separate phase.

Electrochemical measurements were performed at RT using a conventional three-electrode cell. A 0.1 M $HClO_4$ solution saturated with Ar at atmospheric pressure was used as an electrolyte. The glassy carbon electrodes with an applied layer of electrocatalyst powder were used as the working electrodes. The platinum wire was employed as the counter electrode, the Ag/AgCl/KCl saturated electrode – as the reference electrode. The electrochemical surface area of the electrode (ESA) was determined by the quantity of electricity expended for electrochemical adsorption/desorption of atomic hydrogen with input of double layer region [4]. Study of the stability of PtCu NPs was performed using the long-term voltammetric cycling (1000 cycles). Cyclic voltammograms, recorded every 100 cycles (Figure 1), were used to obtain the dependencies of ESA upon the number of cycle for synthesized materials PtCu_seq/C, PtCu_seq-at/C and for the commercial Pt/C material TEC10v30e.

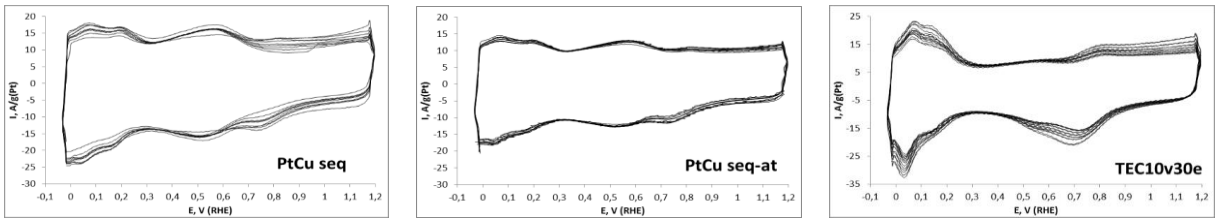

Figure 1. Cyclic voltammograms for materials PtCu_seq/C, PtCu_seq-at/C and for the commercial Pt/C material TEC10v30e recorded during 1000 cycles.

Structural characterization of the synthesized PtCu NPs after two months storage was performed by Pt L_3- and Cu *K*-edge EXAFS. The spectra were measured at the μSpot beamline of the BESSY-II SRF (Berlin, Germany). Mean electron current of a storage ring was maintained during experiment at 300 mA. The measurements were performed in the transmission mode utilizing a Si(111) channel-cut monochromator, two ionization chambers and a diode for reference channel. The photon energy scanning steps were adjusted to δE = 1.0 eV and δk = 0.05 $Å^{-1}$ in the XANES and EXAFS respectively, where E is the energy of incident radiation and k is the photoelectron wavenumber.

The processing of EXAFS in bimetallic NPs requires a large number of structural parameters. Because of the correlations among them, the best-fit set of parameters, obtained from the condition of *R*-factor minimum, may differ significantly from the "real" set since the model used for the fit never includes all contributions, which determine the spectrum fine structure. As a result, the effect of unaccounted contributions is redistributed over the values of correlating parameters in the used model, giving instabilities in the fit parameters depending upon the used Δk intervals and k-weights for $\chi^{exp}(k)$ in FT procedure. To reduce the effect of these correlations, the fitting technique of [5] was implemented, which gives the values of structural parameters using different Δk and k-weights.

Fit of the Fourier-transforms of EXAFS – $F(R)$, was performed using the expressions for $\chi(k)$ based on the qualitative analysis of $F(R)$ in PtCu/C and XRD data:

$$\chi_{\mathrm{Pt}}(k) = N_{\mathrm{Pt-Pt}} \cdot \chi_{\mathrm{Pt-Pt}} + N_{\mathrm{Pt-Cu}} \cdot \chi_{\mathrm{Pt-Cu}}; \quad (1)$$

$$\chi_{\mathrm{Cu}}(k) = \xi_1 \cdot \left(N_{\mathrm{Cu-Cu}} \cdot \chi_{\mathrm{Cu-Cu}} + N_{\mathrm{Cu-Pt}} \cdot \chi_{\mathrm{Cu-Pt}}\right) + \xi_2 \cdot N_{\mathrm{Cu-O,C}} \cdot \chi_{\mathrm{Cu-O,C}}, \quad (2)$$

where $\chi_{\mathrm{A-B}}$ –contribution of one atomic pair A-B (A, B denote Pt or Cu); $\chi_{\mathrm{Cu-O,C}}$ – contribution of interaction of Cu with light atoms O, C; ξ_1, ξ_2 – the fractions of Cu atoms interacting with metal atoms and with light atoms respectively ($\xi_1 + \xi_2 > 1$, since a part of ξ_1 atoms interact also with O, C atoms and a part of ξ_2 atoms interact also with metal ones). Therefore, the independently varied parameters were: amplitudes of each term in (1) and (2), corresponding Debye-Waller parameters ($\sigma^2_{\mathrm{A-B}}$), and distances ($R_{\mathrm{A-B}}$). The fit gave the coincidence of parameters: $R_{\mathrm{Pt-Cu}} \approx R_{\mathrm{Cu-Pt}}$ (up to 0.01Å) and $\sigma^2_{\mathrm{Pt-Cu}} \approx \sigma^2_{\mathrm{Cu-Pt}}$. The last is quite a random, but obtained reasonable for RT values of σ^2 indicate that the fit models (1), (2) enabled to account for Pt and Cu local structures in the sample. Parameters of the third term in (2) are less informative for PtCu NPs structure, however, the obtained value $R_{\mathrm{Cu-O,C}}$ = 1.93 Å is in agreement with the Cu-O distance in copper oxide. Therefore, in Table 1 the values of the following parameters are presented: $N_{\mathrm{Pt-Pt}}$, $N_{\mathrm{Pt-Cu}}$, $\xi_1 \cdot N_{\mathrm{Cu-Pt}}$, $\xi_1 \cdot N_{\mathrm{Cu-Cu}}$, $R_{\mathrm{Pt-Pt}}$, $R_{\mathrm{Pt-Cu}}$, $R_{\mathrm{Cu-Cu}}$, $\sigma^2_{\mathrm{Pt-Pt}}$, $\sigma^2_{\mathrm{Pt-Cu}}$, $\sigma^2_{\mathrm{Cu-Cu}}$. The fit quality, obtained by this set of parameters, is characterized by the values of *R*-factors ≤ 0.015 for both Pt L_3- and Cu *K*-EXAFS, which were calculated for Δk (3.0 – 15.7 Å^{-1}) and $k^{n=2}$.

Table 1. Parameters of Pt and Cu local atomic structure in materials PtCu/C.

Material	$N_{\mathrm{Pt-Pt}}$	$N_{\mathrm{Pt-Cu}}$	$\xi_1 \cdot N_{\mathrm{Cu-Cu}}$	$\xi_1 \cdot N_{\mathrm{Cu-Pt}}$	$R_{\mathrm{Pt-Pt}}$	$R_{\mathrm{Pt-Cu}}$	$R_{\mathrm{Cu-Cu}}$	$\sigma^2_{\mathrm{Pt-Pt}}$	$\sigma^2_{\mathrm{Pt-Cu}}$	$\sigma^2_{\mathrm{Cu-Cu}}$
PtCu_sim/C	6.6	4.5	2.9	4.0	2.73	2.64	2.55	0.006	0.016	0.009
PtCu_sim-at/C	7.4	2.6	1.5	6.6	2.73	2.66	2.61	0.007	0.016	0.010
PtCu_seq/C	8.4	2.5	3.5	2.2	2.75	2.62	2.54	0.006	0.015	0.010
PtCu_seq-at/C	8.8	2.3	3.0	4.8	2.75	2.66	2.57	0.006	0.016	0.009

3. Discussion and conclusions

Broad peaks at 0.5 V (Fig. 1) are associated with the oxidation/reduction of functional groups on the carbon support surface [6]. The absence of anodic peaks corresponding to pure Cu dissolution (0.2 - 0.3 V) or Cu dissolution from the PtCu alloy (0.6 - 0.8 V) on the cyclic voltammograms for the materials PtCu_seq/C and PtCu_seq-at/C indirectly confirms the absence of the Cu/electrolyte interface.

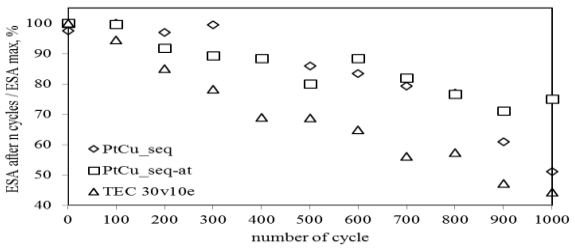

Figure 2. The dependencies of ESA upon the number of cycle for materials PtCu_seq/C (diamonds), PtCu_seq-at/C (squares) and for the commercial Pt/C material TEC10v30e (triangles).

The study of changes in the ESA of catalysts in the process of long-term cycling enabled to compare their morphological stability. Figure 2 shows the different decrease of the ESA value in the considered samples with the increase of the number of cycle. The ESA of PtCu_seq/C electrocatalyst decreased after 1000 cycles by 49% from the maximum value of 36 to 18.6 m^2/g (Pt). Meanwhile, one can conclude that stability of PtCu NPs increases after acid treatment, since for PtCu_seq-at/C material the ESA decreased after 1000 cycles only by 30% from the maximum value of 28 to 20 m^2/g (Pt). For comparison, the stability of the commercial Pt/C material TEC10v30e was also studied: the ESA for this material decreased by 56% from its maximum value of 80 to 35.5 m^2/g after a similar test. Thus, one can see that the commercial Pt/C catalyst degraded significantly faster in comparison with prepared PtCu_seq/C and PtCu_seq-at/C catalysts.

3.1. Cluster modeling of PtCu nanoparticles

The study of averaging over the sizes of PtMe NPs and over the Pt:Me ratio in them [5] enabled to conclude that EXAFS derived structural parameters can be considered as the characteristics of the mean PtMe NP, representative for the PtMe/C catalyst, prepared by one of the considered methods. Meanwhile, to determine the relationship between the synthesis conditions – atomic structure –

electrochemical performances of these materials, it is necessary to visualize the character of components distribution over the volume of NP in correspondence with the values of the local structure parameters derived from EXAFS.

To suggest the models of NPs in materials PtCu/C the method of atomic cluster simulations was implemented using the clusters size D = 8 nm according to TEM data. The comparison of $F(R)$ of Pt L_3- and Cu K- EXAFS of the studied materials with the corresponding $F(R)$ of Pt and Cu foils in the extended R-range (up to ~6.0 Å) enables to conclude, that the cluster models of PtCu NPs structure can be generated using the *fcc* cooper cluster, replacing Cu atoms by Pt ones. The placement of atoms in the cluster was performed by fitting the parameters of radial distribution function of Pt and Cu atoms so as to match the values of EXAFS derived parameters: $N_{\text{Pt-Pt}}$, $N_{\text{Pt-Cu}}$ and the ratio $N_{\text{Cu-Cu}}/N_{\text{Cu-Pt}}$ (since ξ_1 and ξ_2 are undetermined). Cu:Pt ratios obtained by XRF method were used as the boundaries for Cu:Pt ratios in generated clusters: $\text{Cu}^{\text{model}}:\text{Pt}^{\text{model}} < \text{Cu}^{\text{XRF}}:\text{Pt}^{\text{XRF}}$, because a part of Cu atoms can exists in oxide states, independently from NPs. By this technique, the models of NPs in materials PtCu/C were generated (Figures 3, 4). These models show that the components distribution in NPs PtCu_sim corresponds to homogeneous solid solution with Cu:Pt ratio ~0.7 (XRF: 0.9) (Figure 3a), while in PtCu_seq the core-shell structure is realized with Cu:Pt ratio ~0.5 (XRF: 0.7) (Figure 4a). After acid treatment, NPs PtCu_sim-at contain a thin (~one-two atomic layers) Pt-shell corresponding to Cu:Pt ratio ~0.35 (XRF: 0.45) (Figure 3b). The acid treatment of PtCu_seq/C removes Cu cores of NPs with discontinuous shells, forming pure Pt NPs. This is reflected in the relative thickening of the Pt shell in the cluster model of the mean PtCu NP with fixed size, corresponding to Cu:Pt ratio ~0.3 (XRF: 0.4) (Figure 4b). The smearing of the boundary of Cu-core in Figure 4b can be caused by the atoms diffusion due to acid treatment and two months storage of materials, leading to the structural changes. The suggested models are only the possible ones, but the obtained character of components distribution is rather stable within the accuracy (≤ 7%) of N determination by the used processing of EXAFS [5]. To solve the problem of stability and unambiguity of the generated models of NPs the used technique of visualization needs further improvement.

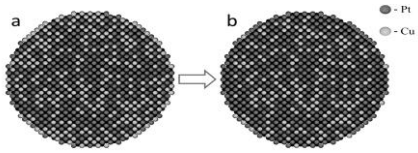

Figure 3. Slices of the atomic clusters modeling NPs in PtCu_sim/C (a) and PtCu_sim-at/C (b).

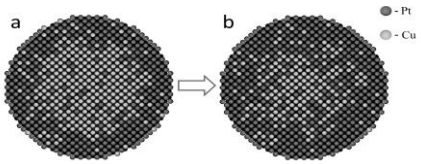

Figure 4. Slices of the atomic clusters modeling NPs in PtCu_seq/C (a) and PtCu_seq-at/C (b).

4. Acknowledgements
The work was supported by Grant 213.01.-07.2014/10ППЧВГ of Southern federal university. Authors are thankful to I. Zizak (INOT, Helmholtz-Zentrum Berlin) for the help during EXAFS measurements.

5. References

[1] Sankar M, Dimitratos N, Miedziak PJ, Wells PP, Kiely CJ and Hutchings GJ. 2012 *Chem. Soc. Rev.* **41** 8099; Russell A E and Rose A. 2004 *Chem. Rev.* **104** 4613–35.
[2] Xu Y, Chen L, Wang X, Yao W and Zhang Q. 2015 *Nanoscale* **7** 10559–83.
[3] Guterman VE, Lastovina TA, Belenov SV, Tabachkova NY, Vlasenko VG, Khodos I and Balakshina EN. 2014 *J. Solid State Electrochem.* **18** 1307-17.
[4] Schulenburg H, Durst J, Muller E, Wokaun A and Scherer GG. 2010 *J. Electroanal. Chem.* **642** 52-60.
[5] Pryadchenko VV, Srabionyan VV, Mikheykina EB, Avakyan LA, Murzin VY, Zubavichus YV, Zizak I, Guterman VE and Bugaev LA. 2015 *J. Phys. Chem. C* **119** 3217-27; Srabionyan VV, Bugaev AL, Pryadchenko VV, Avakyan LA, van Bokhoven JA and Bugaev LA. 2014 *J. Phys. Chem. Solids* **75** 470-6.
[6] Antolini E. 2009 *Appl. Catal. B Environ.* **88** 1–24.